Geophysical Research Letters

RESEARCH LETTER
10.1029/2019GL083753

On the Role of Reduced Air Density Along the Lightning Leader Path to Ground in Increasing X-Ray Production Relative to Normal Atmospheric Conditions

M. D. Tran[1,2], I. Kereszy[1,3], V. A. Rakov[1,4], and J. R. Dwyer[5]

[1]Department of Electrical and Computer Engineering, University of Florida, Gainesville, FL, USA, [2]Now at Rhombus Power Inc., Moffett Field, CA, USA, [3]Department of Physics, University of Florida, Gainesville, FL, USA, [4]Moscow Institute of Electronics and Mathematics, National Research University Higher School of Economics, Moscow, Russia, [5]Department of Physics and Space Science Center (EOS), University of New Hampshire, Durham, NH, USA

Abstract Mallick et al. (2012, https://doi.org/10.1029/2012JD017555) discovered that subsequent-stroke leaders in natural negative lightning could be more prolific producers of hard X-rays and gamma rays than the first-stroke leader in the same flash. However, they had no optical records to confirm that their subsequent leaders followed the same path to ground as the first leader, as opposed to forging a new path to ground through cold air. In this paper, we present new observations, including optical data, showing that a second stroke produced more detectable X-ray pulses than the first stroke, with both strokes following the same channel to ground. Additionally, we present data for the fifth stroke from a different flash, which show the occurrence of X-ray emission at the onset of the common streamer zone between the hot channels of the downward negative dart-stepped leader and upward positive connecting leader. However, there were no detectable X-rays associated with negative leader steps.

Plain Language Summary Cloud-to-ground lightning flashes are each typically composed of 3 to 5 strokes. First stroke necessarily develops in virgin (cold) air, while subsequent strokes often retrace the remnants of the channel(s) of preceding stroke(s). Lightning is known to produce hard X-rays during the initial (leader) stage of each of its strokes. Traditionally, first-stroke leaders were thought to be the main producers of X-rays, and subsequent-stroke leaders (developing in warm, low-density air) were thought to be less active X-ray producers. Mallick et al. (2012) observed subsequent-stroke leaders that were more prolific producers of X-rays than the first-stroke leader in the same flash. However, they had no high-speed video images to confirm that their subsequent leaders followed the same path to ground as the first leader, as opposed to forging a new path to ground through cold air. We present new observations, including high-speed video images, showing that a second stroke produced more detectable X-ray pulses than the first stroke, with both strokes following the same channel to ground. Additionally, we present data for a subsequent stroke from a different flash, which show the rarely observed occurrence of significant X-ray emission at the time of attachment of that stroke to the ground.

Key Points:
- Lightning leaders in previously created but decayed (cooled down) channels can produce more detectable X-rays than the first leader
- The friction curve for air at 3000 K allows all electrons to run away in fields exceeding 3 to 4 MV/m versus 30 to 40 MV/m in cold air
- X-ray emission was observed at the time of collision of opposite-polarity streamers but not at the time of stepping

Supporting Information:
- Supporting Information S1

Correspondence to:
V. A. Rakov,
rakov@ece.ufl.edu

Citation:
Tran, M. D., Kereszy, I., Rakov, V. A., & Dwyer, J. R. (2019). On the role of reduced air density along the lightning leader path to ground in increasing X-ray production relative to normal atmospheric conditions. *Geophysical Research Letters*, *46*, 9252–9260. https://doi.org/10.1029/2019GL083753

Received 16 MAY 2019
Accepted 1 AUG 2019
Accepted article online 05 AUG 2019
Published online 11 AUG 2019
Corrected 22 AUG 2019

This article was corrected on 22 AUG 2019. See the end of the full text for details.

1. Introduction

Lightning leaders are often accompanied by detectable hard X-ray and gamma ray emissions. In this paper, for brevity we refer to any energetic radiation associated with lightning leaders as *X-rays*, regardless of their energies and the details of their production mechanism. A number of studies have shown that both natural (e.g., Mallick et al., 2012; Moore et al., 2001) and triggered (e.g., Dwyer et al., 2004) lightning can produce X-ray emissions. Stepped leaders, dart-stepped leaders, and dart leaders have all been observed to emit X-ray photons with energies in the 30- to 250-keV range and even in the megaelectron volt range.

At present, the only viable mechanism for producing energetic radiation by lightning involves runaway electrons that gain more energy from the electric field between collisions than they lose by collision with air molecules. High-energy electrons are slowed down or deflected as they pass near atoms due to the electric fields of the atom and the electron emits X-rays in the process. This is referred to as bremsstrahlung (i.e., braking radiation). It is likely that X-ray emissions from leaders are associated with the cold runaway (also known as thermal runaway), in which very strong local electric fields allow some free electrons from the ambient background distribution to run away to higher energies.

Mallick et al. (2012) discovered that subsequent-stroke leaders in natural negative lightning could be more prolific producers of X-rays than the first-stroke leader in the same flash, even when the NLDN (National

Lightning Detection Network) reported peak current for subsequent stroke is comparable to or lower than that for the first one. In their study, five out of seven subsequent stroke leaders produced more detectable X-ray pulses than their corresponding first-stroke leaders. They used the relatively short subsequent-leader durations measured in their electric field and electric field derivative records to argue that their subsequent leaders followed the same path to ground as the first leader, as opposed to deviating from the previously formed channel and forging a new path to ground through cold air. The most pronounced example from that study is shown in Figure S1 in the supporting information accompanying this paper, where leaders of strokes 1 and 3 of a negative flash are seen to produce 19 and 109 discernible X-ray pulses, respectively. These two strokes had similar peak currents (50 and 55 kA, respectively) and were inferred to occur in the same channel. The leader of stroke 2 produced only three discernible pulses, but its peak current was about a factor of 2 lower than for strokes 1 and 3.

Mallick et al. (2012) attributed their finding to the fact that normal subsequent leaders traverse channels whose air density is considerably lower than that of the virgin air in which first-stroke leaders have to develop. Their implicit assumption was that the only difference between the first- and subsequent-leader paths in their study was the air temperature (ambient for first leaders vs. about 3000 K for subsequent leaders), with the total particle density at 1-atm pressure for the latter being about an order of magnitude lower than for the former (Uman & Voshall, 1968).

In this paper, we present new observations of X-ray production by first- and second-stroke leaders in the same flash, including optical data that confirm that both leaders followed the same path to ground. The possible role of reduced air density along the lightning leader path to ground in increasing X-ray production relative to normal atmospheric conditions is discussed. Additionally, we present data for the fifth stroke from a different flash, which show the occurrence of pronounced X-ray emission at the onset of the common streamer zone between the hot channels of the downward negative dart-stepped leader and upward positive connecting leader but no detectable X-rays associated with negative leader steps.

2. Instrumentation and Methodology

The optical, electric field (E), electric field derivative (dE/dt), and X-ray data were obtained in 2013–2015 at the Lightning Observatory in Gainesville (LOG), which is located on the roof of the five-story New Engineering Building on the University of Florida campus. X-rays were recorded by the same instrument as was used by Mallick et al. (2012). The high-speed video images of lightning channels were captured using the Megaspeed HHC-X2 high-speed video camera. The framing rate was 1,000 frames per second (1-ms exposure time with essentially zero dead time). More detailed information on our measuring systems is found in Text S1 in the supporting information accompanying this paper.

Using the X-ray detector, Mallick et al. (2012) estimated the occurrence of detectable background (not lightning related) X-rays to be 1 count in 8 ms, or 0.125 counts per millisecond. The probability of observing k background events in a given time interval can be estimated using the Poisson distribution (e.g., McClave & Dietrich, 1979, p. 143):

$$P(k) = \frac{e^{-\lambda}\lambda^{k}}{k!},$$

where λ is the known average number of background X-ray pulses in a given time interval and k is the observed number of X-ray pulses in that interval. Following Mallick et al. (2012), we attribute X-ray pulses to first or subsequent leader if the X-ray emission occurs within 2 ms prior to the corresponding return stroke onset. With the previously estimated background rate of X-ray pulse occurrence (0.25 in a 2-ms interval), the probabilities that 1, 2, or 3 pulses occurred within 2 ms due to background are 0.194, 0.024, and 0.002, respectively. For four or more pulses this probability is <0.0001 (vanishingly small; note that we observed up to 62 X-ray pulses associated with a single leader).

3. Observations and Analysis

In the summers of 2013, 2014, and 2015, we recorded 12 flashes that had at least one stroke whose leader produced detectable X-rays. There were a total of 71 strokes (12 first and 59 subsequent) that were identified in the LOG electric field records, but three of those (all subsequent) were not recorded by the NLDN. All 12 first strokes

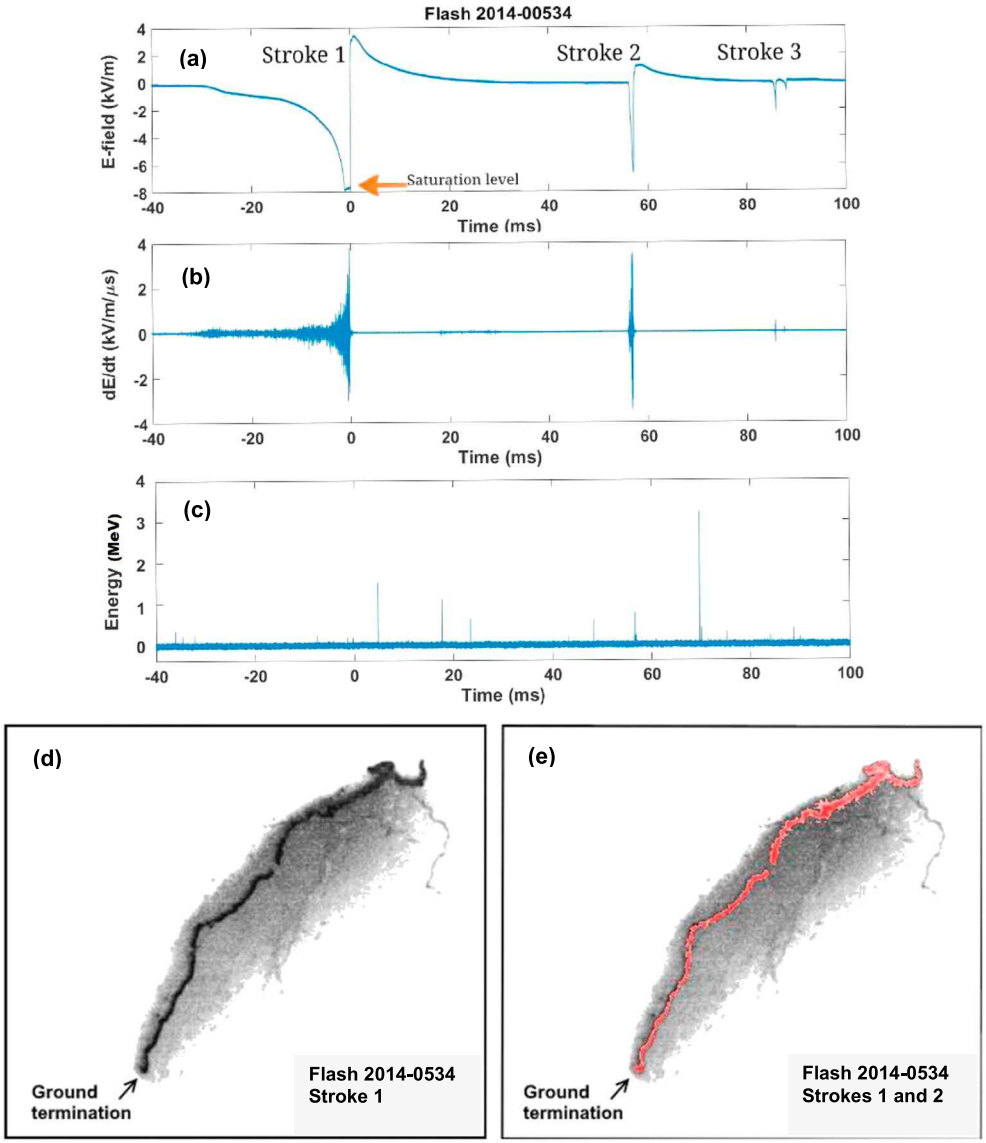

Figure 1. Three-stroke Flash 2014-00534. (a) Electric field, (b) dE/dt, and (c) X-ray records for the entire flash, (d) channel of stroke 1, (e) channel of stroke 2 (in red) overlaid on the channel of stroke 1 (in black), with the latter channel being shown in (d). The two channels appear to be identical (indistinguishable in the superposition shown in e). Stroke 3 also developed in the same channel (not shown here) but produced no detectable X-rays; $t = 0$ corresponds to the onset of the return-stroke process of stroke 1. The largest pulses in (c) are associated with background X-ray emissions; the X-ray pulses associated with leaders of strokes 1 and 2 are labeled in Figures 2c and 2f, respectively.

in our study have produced X-rays, while only 12 (20%) subsequent strokes emitted detectable X-rays, with 2 (17%) of the 12 subsequent strokes producing more X-rays than the associated first stroke, for one of which we obtained optical data. For comparison, as noted in section 1, five (71%) of the seven subsequent strokes in Mallick et al.'s (2012) study produced more detectable X-rays than the corresponding first stroke.

In section 3.1, we present Flash 2014-00534, in which stroke 2 was more prolific X-ray producer than stroke 1. The occurrence of an X-ray pulse at the onset of the common streamer zone during the attachment process in stroke 5 of Flash 2014-00530 is discussed in section 3.2. Further analysis of how our findings compare with those of Mallick et al. (2012) can be found in Text S1 in the supporting information accompanying this paper.

3.1. Flash 2014-00534

On 25 May 2014 we recorded a three-stroke negative cloud-to-ground flash whose ground strike point was between 0.4 and 0.5 km from LOG. The electric field, dE/dt, and X-ray records for the entire flash are

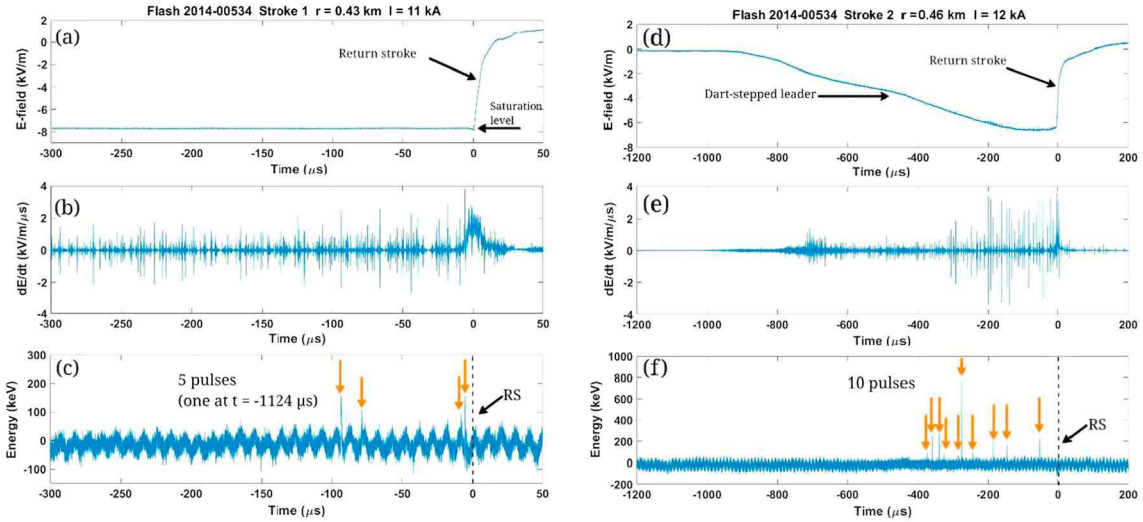

Figure 2. Flash 2014-00534. (a) Electric field, (b) d*E*/d*t*, and (c) X-ray records for stroke 1; (d), (e), and (f) are the same as (a), (b), and (c), respectively, but for stroke 2. Return stroke in each case occurred at $t = 0$. Vertical orange arrows in (c) and (f) point to X-ray pulses. One X-ray pulse that occurred at $t = -1{,}124$ μs, outside of the frame of (c), had a peak of 178 keV.

shown in Figures 1a–1c, and the optical images of strokes 1 and 2 are shown in Figures 1d and 1e. All three leaders followed the same path to ground, as seen in our optical records, but only the leaders of the first two strokes produced detectable X-rays. The first stroke produced five X-ray pulses and the second stroke produced 10 X-ray pulses (see Figure 2). The NLDN only reported the first two strokes with peak currents of 11 and 12 kA for the first and second strokes, respectively. The corresponding NLDN-reported distances were 430 and 460 m, with the difference being due to NLDN location errors (since both strokes followed optically the same channel; see Figures 1d and 1e). Thus, the second stroke followed the same channel to ground, had a peak current that was similar to that of the first stroke, and produced twice as many (10 vs. 5) detectable X-ray pulses. The difference is not very large (just a factor of 2), but in the case presented in Figure S1 stroke 3 produced 109 detectable X-ray pulses versus 19 produced by stroke 1 (the difference is a factor of 5.7). It is important to note that in both cases the "source intensity" (represented by peak current) and distance to the source for the first stroke and the subsequent stroke were essentially the same.

The optical record of the third stroke (not presented here) shows that it followed the same path to ground as well. As noted above, stroke 3 was not recorded by NLDN nor did it produce detectable X-rays. Note that the magnitude of the electric field signature of stroke 3 is small compared to those of strokes 1 and 2 (see Figure 1a). Since the distance was the same for all three strokes (they shared the same channel), the smaller field signature for stroke 3 suggests a smaller causative current. It is known that strokes with smaller peak currents (which are correlated with leader charge densities) are less likely to both be detected by NLDN and produce detectable X-rays (see Tables S1 and S2 in the supporting information accompanying this paper).

As seen in Figure 2e, the leader of stroke 2 was dart stepped (see pronounced bipolar pulses between about −300 μs and 0; four such pulses, in a different stroke, are marked in Figure 3b). The X-ray pulses marked in Figure 2f appear to coincide with the steps of this dart-stepped leader. However, there are many steps that are not accompanied by detectable X-ray pulses. One possible explanation is that not all X-rays were detectable at LOG because of leader channel tortuosity and directional beaming during bremsstrahlung (Jackson, 1962, p. 514), resulting insufficient photon flux density in the direction of LOG. Another possible (and likely) explanation is that some steps produce X-rays, while others do not. This is further discussed in section 4.

3.2. Flash 2014-00530

Flash 2014-00530 also occurred on 25 May 2014 and contained five negative strokes. The first, second, third, and fifth strokes produced detectable X-rays. Figure 3 shows the electric field, electric field derivative, and X-ray records for the fifth stroke of the flash, which was initiated by a dart-stepped leader. No optical

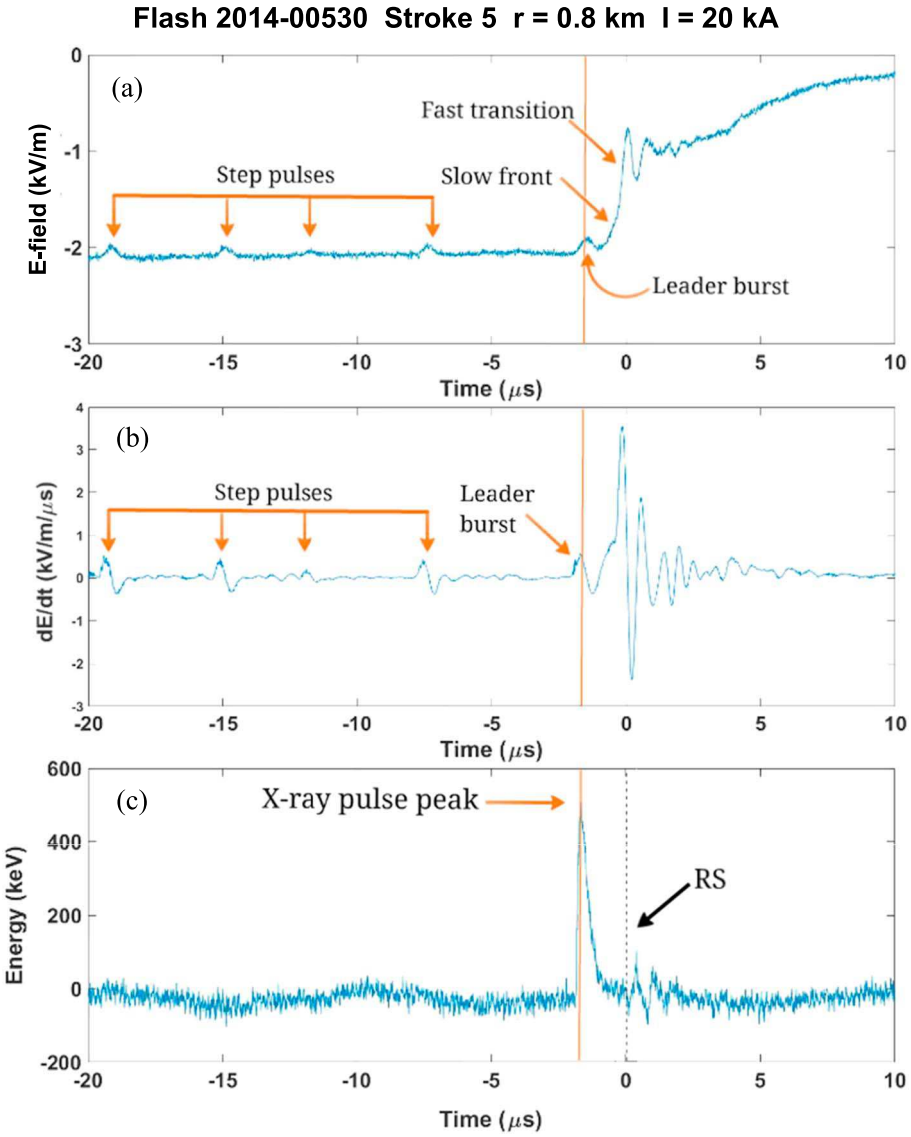

Figure 3. Flash 2014-00530. (a) Electric field, (b) dE/dt, and (c) X-ray records for stroke 5. Only one detectable X-ray pulse was produced by this stroke, which occurred in coincidence with the LB seen at the beginning of the slow front in the dE/dt record. The occurrence of the X-ray pulse at the time of LB suggests that the X-ray emission was associated with the collision of streamer zones of opposite polarity associated with the downward negative leader and upward positive connecting leader. Solid vertical lines in (a), (b), and (c) indicate the position of the leader burst peak in (b). Broken vertical line at $t = 0$ in (c) indicates the position of initial peak of return-stroke electric field waveform in (a).

records are available for this flash, but, judging from (see, for example, Rakov & Uman, 2003, Ch. 4) the leader duration (about 1 ms) and the average interstep interval (about 5 μs or less), both estimated from electric field records, stroke 5 followed a previously created but decayed channel.

The last four step pulses are marked by vertical arrows in Figures 3a and 3b; none of them is accompanied by an X-ray pulse in Figure 3c. The initial part of the return-stroke waveform exhibited the characteristic slow front (SF) followed by the fast transition (FT; see Figure 3a). The beginning of SF is marked by the so-called leader burst (LB), which signifies the beginning of the so-called breakthrough phase (BTP) of the lightning attachment process. The BTP starts when the poorly conducting streamer zones developing ahead of the hot channels of negative downward leader and positive upward connecting leader come in contact and a common streamer zone is formed. Additional information on the BTP is found in the works of Tran and Rakov (2017) and Rakov and Tran (2019) and in references therein. The onset of the LB

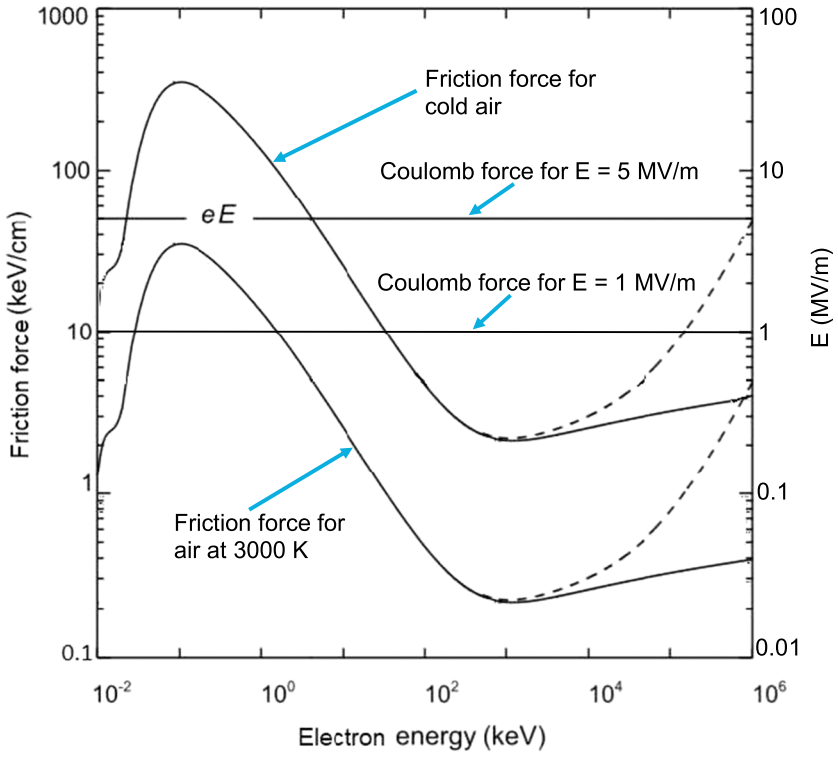

Figure 4. The dynamic friction curves showing the friction force (rate of energy loss) experienced by an electron as a function of electron energy for cold air and for air at 3000 K. The solid-line curve is due to inelastic scattering of the electron with air molecules and the dashed-line part includes the effects of bremsstrahlung emission. The horizontal lines represent the Coulomb force acting on electrons (eE, where E is the electric field intensity and e is the electron charge) corresponding to $E = 1$ MV/m and $E = 5$ MV/m (see the right vertical scale). Electrons can run away to relativistic energies when the Coulomb force is greater than the friction force. For cold air and $E = 5$ MV/m, only electrons with energy greater than 5 keV can run away, while for the air at 3000 K and the same E all electrons can do so. The friction curve for cold air is taken from Dwyer (2004, Figure 1).

corresponds to the collision of opposite polarity streamers, which is expected to produce X-ray bursts (Cooray, Arevalo, et al., 2009). Such bursts were observed in laboratory spark experiments (Kochkin et al., 2012, 2015) and in lightning (Howard et al., 2010). A pronounced X-ray pulse corresponding to LB is seen in Figure 3c. There are only a few records of this kind found in the literature. Note that none of the step pulses seen in Figures 3a and 3b is accompanied by X-rays in Figure 3c, which may be in support of the view (e.g., Mallick et al., 2012) that X-ray emission is not a necessary feature of negative-leader stepping process. Leaders of strokes 1, 2, and 3 produced seven, one, and one X-ray pulses respectively, some of which were associated with steps, but none occurred at the beginning of BTP. Stroke 3 (similar to strokes 4 and 5) followed a previously created channel, while stroke 2 apparently (judging from electric field records) created a new termination on ground. It is interesting that in this flash only one stroke had BTP whose beginning was marked by detectable X-ray emission and that emission was produced in warm, low-density air, not in cold air in which BTP of strokes 1 and 2 had to develop.

4. Discussion and Concluding Remarks

In section 3.1, we presented flash 2014-00534, which contained three strokes, all of which followed the same channel to ground, as unambiguously confirmed by our high-speed video records. Stroke 3 has not produced detectable X-rays and is not further considered here. Stroke 2 developed along the remnants of the channel previously formed by stroke 1 (that is, both strokes occurred at the same distance) and, according to the NLDN, their peak currents were similar, yet stroke 2 produced twice as many X-ray pulses than stroke 1. If we assume that the same channel geometry means approximately the same X-ray emission pattern and, hence, the same relative X-ray flux toward our detector, the reason could the elevated temperature and, hence, lower air density along the path traversed by the second leader, relative to the normal atmospheric

conditions path traversed by the first leader. This explanation was also suggested for similar observations (see, for example, Figure S1 in the supporting information) by Mallick et al. (2012). Indeed, normal subsequent-stroke leaders traverse channels whose temperature is typically 3000 versus 300 K for the virgin air in which first-stroke leaders have to develop. Since the pressure is about the same for the channels of both first- and subsequent-stroke leaders, a factor of 10 difference in temperature leads to a factor of 10 difference in air density as follows from the ideal gas law:

$$PV = nRT, \tag{1}$$

where P is pressure in Pascals, V is volume in cubic meters, n is the number of moles of gas, R is the universal gas constant (8.314 J/[mol·K]), T is the temperature in Kelvins, and n/V is the gas density.

Electrons gain energy as they are accelerated by the electric field and lose energy in collisions with other particles. The rate of energy loss is often represented (e.g., Coleman et al., 2010; Dwyer et al., 2012) by the dynamic friction force that is a function of electron energy, the resultant dependence being referred to as the "friction curve." One can expect that the friction force experienced by the accelerating electrons will be smaller and the mean free path will be longer for the warmer, lower-density channel in front of a subsequent leader traversing the warm remnants of previously formed channel. The mean free path λ (in meters) is given by

$$\lambda = \frac{1}{N\sigma}, \tag{2}$$

where σ is the collision cross section in square meters and N is the air density (i.e., number density) in inverse cubic meters. Since the air density of the channel at 3000 K is 10 times lower than that of the cold air, the mean free path for the former is 10 times longer (688 vs. 68.8 nm). This means that electrons in previously conditioned channels will gain more energy between collisions and will be more likely to run away and contribute to the avalanche growth process than in cold air.

The dynamic friction force $F(\varepsilon)$ can be expressed as (Moss et al., 2006)

$$F(\varepsilon) = \sum_j N_j \sigma_j(\varepsilon) \delta\varepsilon_j \tag{3}$$

where ε is the electron energy. The summation index $\sum_j$ takes on the values of 1, 2, and 3 and represents summation over all the collision processes for nitrogen, oxygen, and argon, respectively, each of which is present in air with partial density N_j. The cross-section $\sigma_j(\varepsilon)$ and associated electron energy loss $\delta\varepsilon_j$ each represent the entirety of all inelastic collision processes for a given gas j.

Since the friction force (for each constituent) is a linear function of air density, a factor of 10 decrease in N leads to a factor of 10 decrease in the friction force. Figure 4 shows the friction force as a function of electron energy (friction curve) for cold air (upper curve) and for air at 3000 K (lower curve). The possibility that the rarefaction of air plays a role in the production of X-rays has been considered by Köhn, Chanrion, Babich, et al. (2018); Köhn,Chanrion, Neubert, (2018).

The Coulomb force equal to the maximum of the friction curve corresponds to the critical (minimum) electric field above which virtually all electrons will run away. Those critical fields (see the right vertical scale) are 30 to 40 MV/m and 3 to 4 MV/m for cold air and air at 3000 K, respectively. The corresponding maxima of the friction force (see the left vertical scale) are 300 to 400 keV/cm and 30 to 40 keV/cm.

It is important to note that the friction curve represents the average friction (average energy loss) experienced by electrons, but since the collisions of individual electrons are stochastic some electrons might experience fewer collisions than the average, gain more energy, and run away even if, according to the friction curve, their initial energy is lower than needed for them to run away in a given electric field (Diniz et al., 2019).

Cooray, Becerra, & Rakov (2009) showed that dart leaders can produce electric field pulses briefly exceeding the threshold corresponding to the peak of the friction curve for warm, low-density air (see the lower curve in Figure 4). Specifically, for a dart leader propagating at 10^7 m/s and prospective return-stroke peak current of 12 kA, the electric field peaks were found to be 0.8, 1.5, and 2.9 MV/m for dart-leader current risetimes of 0.5, 1.0, and 2.0 μs, respectively. The corresponding electric field pulse widths at half-maximum were about 130, 200, and 480 ns. In a follow-up study, Cooray et al. (2010) investigated what channel temperature is

needed for production of runaway electrons by subsequent leaders as a function of the following return-stroke peak current. They have found that a typical subsequent stroke with peak current of 12 kA needs to have its leader follow a previously created but decayed channel with temperature of 2500 K or higher in order for electrons to run away. The second stroke of the flash discussed in section 3.1 (Flash 2014-00534) had a peak current of 12 kA, which is typical for negative subsequent strokes. The time interval between strokes 1 and 2 was about 60 ms, which is expected for multiple-stroke negative flashes. According to Uman and Voshall (1968), the channel temperature after a typical interstroke interval is about 3000 K. Thus, our observations presented in section 3.1 confirm Cooray et al.'s (2010) theoretical prediction that a leader of typical subsequent stroke can produce runaway electrons and, hence, X-ray emission.

In section 3.2, we presented (see Figure 3) a pronounced X-ray pulse that was coincident in time with the LB signifying the beginning of the BTP. The LB process differs from the regular leader step in that the negative corona streamer burst of the former makes contact with the positive streamer zone of the grounded upward connecting leader channel, rather than ending in midair, as in the case of a regular leader step (Rakov & Tran, 2019; Tran & Rakov, 2017). Howard et al. (2010) reported that, in contrast with the SF and FT pulses, the sources of LB pulses exhibited rapid movements and were prolific X-ray producers. X-ray bursts at the time of collision of opposite polarity streamers were predicted by Cooray, Arevalo, et al. (2009) and observed in laboratory spark experiments (Kochkin et al., 2012; Kochkin et al., 2015). Those observations have been followed by a number of modeling efforts (Babich & Bochkov, 2017; Ihaddadene & Celestin, 2015; Kochkin et al., 2016; Köhn et al., 2017; Luque, 2017). Our results presented in section 3.2 confirm the finding of Howard et al. (2010) that the establishment of common streamer zone in negative subsequent strokes of natural lightning can be associated with significant X-ray emission. At the same time, no detectable X-rays were found to be associated with the negative-leader stepping process (see Figure 3), which is known to culminate in an intense negative corona streamer burst. This latter streamer burst has been thought to be the primary source of X-ray emission associated with leader steps. On the other hand, strokes 1, 2, and 3 did produce detectable X-ray pulses associated with leader steps but not with the beginning of BTP. Overall, it appears that X-ray emission may be not a necessary feature of either corona streamer bursts associated with leader steps or collision of opposite polarity streamers at the beginning of lightning attachment process, although insufficient X-ray flux in the direction of the detector could be a factor.

Acknowledgments
This work was supported in part by NSF Grant AGS-1701484. The authors would like to thank Ron Holle and William Brooks of Vaisala for providing NLDN data. All data files related to this paper are found at https://drive.google.com/open?id=1OsB0B8UC98h-AU6svWmf2qY3P25JpYCw.

References

Babich, L., & Bochkov, E. (2017). Numerical simulation of electric field enhancement at the contact of positive and negative streamers in relation to the problem of runaway electron generation in lightning and in long laboratory sparks. *Journal of Physics D: Applied Physics*, *50*(45), 45,5202–45,5208. https://doi.org/10.1088/1361-6463/aa88fd

Coleman, J. J., Roussel-Dupré, R. A., & Triplett, L. (2010). Temporally self-similar electron distribution functions in atmospheric breakdown: The thermal runaway regime. *Journal of Geophysical Research*, *115*, A00E16. https://doi.org/10.1029/2009JA014509

Cooray, V., Arevalo, L., Rahman, M., Dwyer, J. R., & Rassoul, H. (2009). On the possible origin of X-rays in long laboratory sparks. *Journal of Atmospheric and Solar - Terrestrial Physics*, *71*(17–18), 1890–1898. https://doi.org/10.1016/j.jastp.2009.07.010

Cooray, V., Becerra, M., & Rakov, V. A. (2009). On the electric field at the tip of dart leaders in lightning flashes. *Journal of Atmospheric and Solar-Terrestrial Physics*, *71*(12), 1397–1404. https://doi.org/10.1016/j.jastp.2009.06.002

Cooray, V., Dwyer, J. R., Rakov, V. A., & Rahman, M. (2010). On the mechanism of X-ray production by dart leaders of lightning flashes. *Journal of Atmospheric and Solar - Terrestrial Physics*, *72*(11–12), 848–855. https://doi.org/10.1016/j.jastp.2010.04.006

Diniz, G. S., Rutjes, C., Ebert, U., & Ferreira, I. S. (2019). Cold electron runaway below the friction curve. *Journal of Geophysical Research: Atmospheres*, *124*, 189–198. https://doi.org/10.1029/2018JD029178

Dwyer, J. R. (2004). Implications of x-ray emission from lightning. *Geophysical Research Letters*, *31*, L12102. https://doi.org/10.1029/2004GL019795

Dwyer, J. R., Rassoul, H. K., al-Dayeh, M., Caraway, L., Wright, B., Chrest, A., et al. (2004). Measurements of x-ray emission from rocket-triggered lightning. *Geophysical Research Letters*, *31*, L05118. https://doi.org/10.1029/2003GL018770

Dwyer, J. R., Smith, D. M., & Cummer, S. A. (2012). High-energy atmospheric physics: Terrestrial gamma-ray flashes and related phenomena. *Space Science Reviews*, *173*(1-4), 133–196. https://doi.org/10.1007/s11214-012-9894-0

Howard, J., Uman, M. A., Biagi, C., Hill, D., Jerauld, J., Rakov, V. A., et al. (2010). RF and X-ray source locations during the lightning attachment process. *Journal of Geophysical Research*, *115*, D06204. https://doi.org/10.1029/2009JD012055

Ihaddadene, M. A., & Celestin, S. (2015). Increase of the electric field in head-on collisions between negative and positive streamers. *Geophysical Research Letters*, *42*, 5644–5651. https://doi.org/10.1002/2015GL064623

Jackson, J. D. (1962). *Classical electrodynamics*. New York, NY: John Wiley & Sons, Inc.

Kochkin, P. O., Köhn, C., Ebert, U., & van Deursen, L. (2016). Analyzing X-ray emissions from meter-scale negative discharges in ambient air. *Plasma Sources Science and Technology*, *25*, 04,4002–04,4017. https://doi.org/10.1088/0963-0252/25/4/044002

Kochkin, P. O., Nguyen, C. V., van Deursen, A. P. J., & Ebert, U. (2012). Experimental study of hard x-rays emitted from metre-scale positive discharges in air. *Journal of Physics D: Applied Physics*, *45*(42), 42,5202–42,5211. https://doi.org/10.1088/0022-3727/45/42/425202

Kochkin, P. O., van Deursen, A. P. J., & Ebert, U. (2015). Experimental study of hard x-rays emitted from metre-scale negative discharges in air. *Journal of Physics D: Applied Physics*, *48*(2), 02,5205–02,5217. https://doi.org/10.1088/0022-3727/48/2/025205

Köhn, C., Chanrion, O., Babich, L. P., & Neubert, T. (2018). Streamer properties and associated x-rays in perturbed air. *Plasma Sources Science and Technology*, *27*(1), 015017. https://doi.org/10.1088/1361-6595/aaa5d8

Köhn, C., Chanrion, O., & Neubert, T. (2017). Electron acceleration during streamer collisions in air. *Geophysical Research Letters*, *44*, 2604–2613. https://doi.org/10.1002/2016GL072216

Köhn, C., Chanrion, O., & Neubert, T. (2018). High-energy emissions induced by air density fluctuations of discharges. *Geophysical Research Letters*, *45*, 5194–5203. https://doi.org/10.1029/2018GL077788

Luque, A. (2017). Radio frequency electromagnetic radiation from streamer collisions. *Journal of Geophysical Research: Atmospheres*, *122*, 10,497–10,509. https://doi.org/10.1002/2017JD027157

Mallick, S., Rakov, V. A., & Dwyer, J. R. (2012). A study of X-ray emissions from thunderstorms with emphasis on subsequent strokes in natural lightning. *Journal of Geophysical Research*, *117*, D16107. https://doi.org/10.1029/2012JD017555

McClave, J. T., & Dietrich, F. H. (1979). *Statistics*. San Francisco, CA: Dellen Publishing Company.

Moore, C. B., Eack, K. B., & Aulich, G. D. (2001). Energetic radiation associated with lightning stepped-leaders. *Geophysical Research Letters*, *28*(11), 2141–2144. https://doi.org/10.1029/2001GL013140

Moss, G., Pasko, V. P., Liu, N., & Veronis, G. (2006). Monte Carlo model for analysis ofthermal runaway electrons instreamer tipsin transient luminous events and streamer zones of lightning leaders. *Journal of Geophysical Research*, *111*, A02307. https://doi.org/10.1029/2005JA011350

Rakov, V. A., & Tran, M. D. (2019). The breakthrough phase of lightning attachment process: From collision of opposite-polarity streamers to hot-channel connection. *Electric Power Systems Research*, *173*, 122–134. https://doi.org/10.1016/j.epsr.2019.03.018

Rakov, V. A., & Uman, M. A. (2003). *Lightning:Physics and Effects*. New York: Cambridge University Press.

Tran, M. D., & Rakov, V. A. (2017). A study of the ground-attachment process in natural lightning with emphasis on its breakthrough phase. *Nature Scientific Reports*, *7*(1), 15,761–15,773. https://doi.org/10.1038/s41598-017-14842-7

Uman, M. A., & Voshall, R. E. (1968). Time interval between lightning strokes and the initiation of dart leaders. *Journal of Geophysical Research*, *73*(2), 497–506. https://doi.org/10.1029/JB073i002p00497

Erratum

In the originally published version of this article, the Plain Language Summary was published incorrectly. This error has since been corrected, and the present version may be considered the authoritative version of record.